

# MICROSCOPIC ORIGINS OF ENHANCED OUTPUT OF HEUSLER ALLOY CPP-GMR READERS BY AMORPHOUS UNDERLAYER AND CONDUCTIVE OXIDE SPACER

T. NAKATANI<sup>1</sup>, S. LI<sup>1</sup>, Y. SAKURABA<sup>1</sup>, T. T. SASAKI<sup>1</sup>, X. D. XU<sup>1</sup>, H. TAJIRI<sup>2</sup>, T. FURUBAYASHI<sup>1</sup> and K. HONO<sup>1</sup>

1: National Institute for Materials Science

2: Japan Synchrotron Radiation Research Institute

## I. INTRODUCTION

As the read sensor size is decreased, the sensor resistance increases and the electrical noise increases. Therefore, reducing the resistance-area product ( $RA$ ) of sensor film is the central issue for realizing the read sensors for ultrahigh recording density HDDs. All-metallic current-perpendicular-to-plane giant magnetoresistance (CPP-GMR) using highly spin-polarized Co-based Heusler alloys have demonstrated large CPP-GMR ratio over 40% at low  $RA < 0.05 \Omega \mu\text{m}^2$  [1, 2]. This was achieved by annealing single-crystalline Heusler alloy films at high temperature above 500 °C to obtain a high degree of L2<sub>1</sub> or B2 chemical order of Heusler alloys. For the realization of CPP-GMR read sensors, however, achieving large CPP-GMR output using polycrystalline films annealed at a lower temperature (currently, ~300 °C) is important. Recently, Choi *et al.* [3] reported that CPP-GMR ratio of spin-valves using polycrystalline Heusler alloy layers could be improved by inserting thin (< 1 nm) amorphous CoFeBTa underlayer below the Heusler alloy layer. In addition, the non-magnetic spacer layer of CPP-GMR device has a great potential for improving the CPP-GMR value. Especially, a InZnO (IZO) conductive oxide-based spacer layer [5] is promising because of the slightly increased RA to ~0.1  $\Omega \mu\text{m}^2$ , which is optimal for read sensor application for 2 Tbit/in<sup>2</sup> [4], and the improved MR ratio ~25% achieved in practical spin-valve sensor structure.

In this presentation, we review our recent studies to understand the mechanisms of MR enhancements by (i) CoFeBTa amorphous underlayer inserted below Heusler alloy magnetic layer, and (ii) Ag/IZO/Zn spacer layer using synchrotron x-ray diffraction and electron microscopy.

## II. EXPERIMENTAL PROCEDURES

CPP-GMR films were deposited by magnetron sputtering at room temperature. Co<sub>2</sub>(Mn<sub>0.6</sub>Fe<sub>0.4</sub>)Ge (CMFG) Heusler alloy was used for the ferromagnetic layers. The films were annealed at 280 °C or 300 °C for 3 hours and patterned into CPP pillars. The degree of B2 ordering (site ordering between Co and (Mn,Fe)) was measured in 30 nm thick CMFG films by anomalous x-ray diffraction (XRD) near the x-ray energy of the Co-K absorption (~7.7 keV) in a synchrotron facility SPring-8.

## III. RESULTS and DISCUSSION

Figure 1(a) shows the resistance change-area product ( $\Delta RA$ ) of Cu-lead/Ru(1)/CoFe(1)/CoFeBTa(0-1.2)/CMFG(5)/CoFe(0.4)/AgSn(4)/CoFe(0.4)/CMFG(5)/CoFe(1)/Ru cap (thickness in nm) pseudo spin-valve devices annealed at 300 °C. (Co<sub>40</sub>Fe<sub>40</sub>B<sub>20</sub>)<sub>0.93</sub>Ta<sub>7</sub> amorphous underlayer was inserted below the bottom CMFG layer.  $\Delta RA$  increased by inserting the CoFeBTa amorphous underlayer. As shown by the inset of Fig. 1(a), the CPP-GMR device with the CoFeBTa(1.2 nm) insertion showed  $RA = 30 \text{ m}\Omega \mu\text{m}^2$  and MR ratio ( $\Delta R/R$ ) of 25%. As shown in Fig. 1(b), the degree of B2 order measured for 30 nm-CMFG films was higher for the CMFG films with thicker CoFeBTa insertion. Therefore, the increased  $\Delta RA$  by the insertion of CoFeBTa should be originated from the enhanced B2 ordering of CMFG. It is also noteworthy that the degree of B2 order of the top CMFG deposited on the AgSn spacer layer (corresponding to the free layer of bottom-pinned spin-valve) was much lower (~46%) than those of the bottom CMFG deposited on the CoFeBTa underlayer (up to 76%). Thus, improving the degree of B2 order of the top CMFG layer is a key for further increase of CPP-GMR outputs.

Next, we studied the microstructure of CPP-GMR spin-valves with IZO-based spacer layers. Figure 2

shows  $RA$  vs.  $\Delta R/R$  of bottom-pinned spin-valves with Cu/Ta-lead/Ta(2)/Ru(2)/IrMn(6)/CoFe(2.6)/Ru(0.8)/CoFe(0.6)/CoFeBTa(0.8)/CMFG(2.5)/CoFe(0.4)/spacer/CoFe(0.4)/CMFG(4)/CoFe(1)/Ru cap structure annealed at 280 °C. By using Ag(Sn)/IZO/Zn spacer layers, both  $\Delta R/R$  and  $RA$  increased compared to the spin-valve with the metallic AgSn(4) spacer layer. Figures 3 (a)-(b) shows the elemental mappings of In, Zn and Ag, respectively in the spin-valve film with Ag(0.4)/IZO(1.6)/Zn(0.8) spacer layer by energy dispersive x-ray spectrometry in scanning transmission microscopy, Ag shows an inhomogeneous concentration distribution in the position of the IZO layer. Thus, the distribution of the CPP electric current is expected to be inhomogeneous similar to that in current-confined-path spacer layer. Furthermore, as shown by the depth concentration profiles in Fig. 3(e), Mn is diffused into the spacer layer. The Mn impurity in spacer layer may cause a spin-flip scattering, thus it should reduce the CPP-GMR output. Therefore, suppressing the Mn diffusion to IZO-based spacer should improve the CPP-GMR sensor output.

## References

- [1] Sakuraba *et al.* Appl. Phys. Lett. 101, 252408 (2012). [2] Li *et al.* Appl. Phys. Lett. 103, 042405 (2013). [3] Choi *et al.* Appl. Phys. Express 10, 013006 (2017). [4] Nakatani *et al.* Appl. Phys. Express 8, 093003 (2015). [5] Takagishi *et al.* IEEE Trans. Magn. 46, 2086 (2010).

## Figures

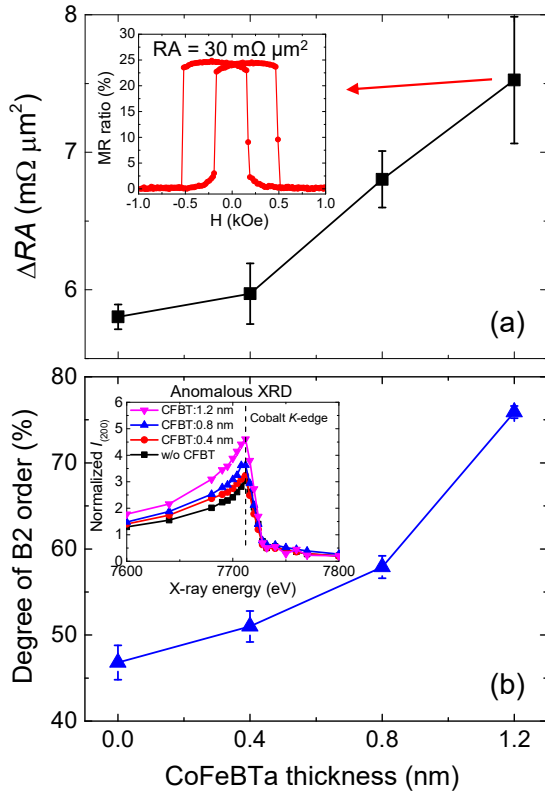


Fig. 1 (a)  $\Delta RA$  and (b) degree of B2 order of CMFG film for various thickness of CoFeBTa underlayer.

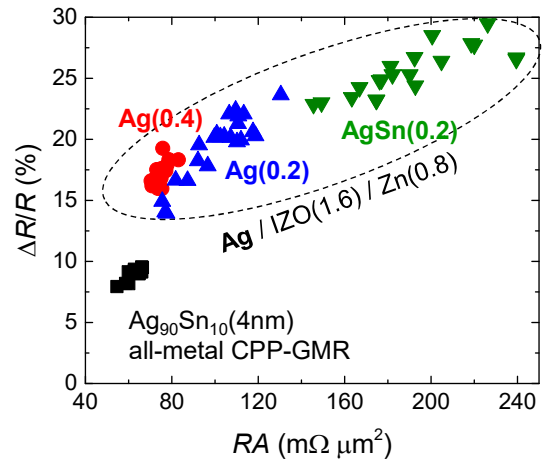


Fig. 2  $RA$ - $\Delta R/R$  of spin-valves with Ag(Sn)/IZO/Zn and AgSn spacer layers.

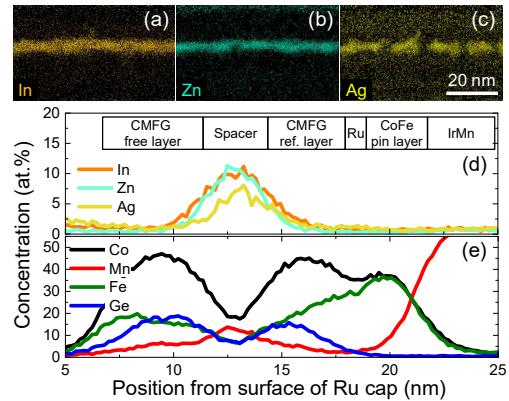


Fig. 3 Elemental concentration maps and profiles in spin-valves with Ag(0.4)/IZO(1.6)/Zn(0.8) spacer layer.